

Traveling waves in a continuum model of schooling swimmers

Anand U. Oza*

*Department of Mathematical Sciences & Center for Applied Mathematics and Statistics,
New Jersey Institute of Technology, Cullimore Hall, Newark, NJ 07102, USA*

Eva Kanso

*Department of Aerospace and Mechanical Engineering & Department of Physics and Astronomy,
University of Southern California, 3650 McClintock Avenue, Los Angeles, CA 90089, USA*

Michael J. Shelley

*Courant Institute of Mathematical Sciences, 251 Mercer Street, New York, NY 10012, USA and
Center for Computational Biology, Flatiron Institute, 162 Fifth Avenue, New York, NY 10010, USA*

(Dated: July 9, 2025)

The complex formations exhibited by schooling fish have long been the object of fascination for biologists and physicists. However, the physical and sensory mechanisms leading to organized collective behavior remain elusive. On the physical side in particular, it is unknown how the flows generated by individual fish influence the collective patterns that emerge in large schools. To address this question, we here present a continuum theory for a school of swimmers in an inline formation. The swimmers are modeled as flapping wings that interact through temporally nonlocal hydrodynamic forces, as arise when one swimmer moves through the lingering vortex wakes shed by others, leading to a system of time-delay-differential equations. Through coarse-graining, we derive a system of partial differential equations for the evolution of swimmer density and collective vorticity-induced hydrodynamic force. Linear stability analysis of the governing equations shows that there is a range of swimmer densities for which the uniform (constant-density) state is unstable to perturbations. Numerical simulations reveal families of stable traveling wave solutions, where a uniform school destabilizes into a collection of densely populated “sub-schools” separated by relatively sparse regions that move as a propagating wave. We find that distinct propagating waves may be stable for the same set of kinematic parameters. Generally, our results show that temporally nonlocal hydrodynamic interactions can lead to rich collective behavior in schools of swimmers.

I. INTRODUCTION

The complex dynamics of animal collectives such as fish schools offers a beautiful visualization of non-equilibrium collective behavior [1]. A fish school is an archetype of an active matter system, as the individual organisms consume energy in order to self-propel and interact with each other [2]. The mechanisms by which large groups of fish generate and sustain organized collective locomotion has long fascinated scientists [3, 4], one goal being to uncover their fundamental underlying biological principles and use them towards potential engineering applications, for example designing swarms of biomimetic underwater vehicles [5].

Much of the prior research has focused on the behavioral mechanisms by which fish interact with each other while schooling [6, 7]. Experimental studies of different fish species in controlled environments have sought to uncover interaction rules that govern how fish move and orient themselves with respect to each other [8–13]. These studies are complemented by a variety of theoretical models that seek to capture the collective phenomena observed in biological systems. Discrete models, such as the seminal Viscek model [14] and variants

thereof (e.g. [15–17]), posit equations of motion for the coupled positional and orientational dynamics of interacting agents that sense each other and respond accordingly while being perturbed by stochastic noise. Continuum models have the advantage of being more amenable to analysis, and are biologically relevant when a collective contains a large number of individuals. For example, the celebrated Toner-Tu continuum partial differential equation (PDE) theory [18–20] is a coarse-graining of the Viscek model, and has motivated other more sophisticated theories (e.g. [21, 22]). Partial integro-differential equations have been used to model spatially nonlocal sensory interactions [23–26], wherein the constituents sense and thus interact with each other over long ranges. Despite their successes, these spatially nonlocal models do not account for temporally nonlocal interactions between constituents. Specifically, swimming fish generate flow structures that persist over spatial and temporal scales relevant to physical interactions within a school [27], yet modeling these interactions remains challenging due to the inherently non-local and non-instantaneous nature of these flows.

A substantial body of research has demonstrated that hydrodynamic interactions are important in mediating schooling behavior [28]. For example, studies have demonstrated that fish exert less energy while swimming in a school than they do in isolation [29–31], especially in the turbulent flow conditions characteristic of

* oza@njit.edu

relatively fast-moving schools [32]. Hydrodynamic considerations have been used to rationalize the emergence of particular schooling formations over others in a water tank [33]. In order to isolate hydrodynamic effects, recent experiments have been performed in which fish are replaced by freely-swimming wings, whose vertical (periodic) flapping motion is prescribed but horizontal motion is determined by the balance of hydrodynamic thrust and drag forces. These experiments have shown that a linear periodic array of flapping wings can move faster than a single wing [34], and that pairs of wings in an in-line [35] or staggered [36, 37] formation spontaneously adopt steady “schooling modes,” wherein the pair translates at constant velocity while maintaining a fixed separation distance. Such modes persist even if the wings’ flapping amplitudes and frequencies are incommensurate [38]. Groups of more wings in an in-line formation exhibit flow-induced instabilities, wherein disturbances to the leader wing progressively amplify as they propagate downstream and can cause collisions between the trailing wings [39].

Theoretical models have been developed to describe hydrodynamic interactions between schooling swimmers in relatively high-Reynolds number flows. Models that account for far-field hydrodynamic effects, wherein each swimmer is modeled as a dipole [40, 41], have been used to demonstrate that swimmers adopt different schooling modes due to hydrodynamic interactions [42], and that swimming collectives undergo phase transitions when in confinement [43]. Near-field hydrodynamic interactions, which are due to the vortices generated by fish as they swim [27], have been modeled using a generalized thin-airfoil theory [44, 45], wherein the periodic wake generated by a flapping plate is assumed to be flat [35, 46]. The vortices shed by fish have been modeled explicitly using point-vortex models, first in Refs. [47, 48] and later generalized in Ref. [49], which were used to compare the hydrodynamic thrust and efficiency of different schooling formations. Numerical simulations using a vortex sheet method have been used to assess the hydrodynamic interactions between pairs [50, 51] and larger collectives [52, 53] of flapping plates in the limit of infinite Reynolds number.

However, there is currently no continuum description of swimmers that generate and interact through a relatively high-Reynolds number flow, a necessary step towards simulating the large fish schools observed in nature. The difficulty is that the hydrodynamic interactions between swimming fish are *temporally nonlocal*: while small-scale objects such as bacteria [54] or cilia [55] generate a low-Reynolds number (Stokes) flow that can be readily incorporated into continuum models because the interactions between constituents are instantaneous, fish swim at higher Reynolds number and thus generate vortical flow structures that persist over a timescale τ that is often comparable to the timescale d/u_0 over which fish interact, d and u_0 being the typical distance between and velocity of the fish, respectively.

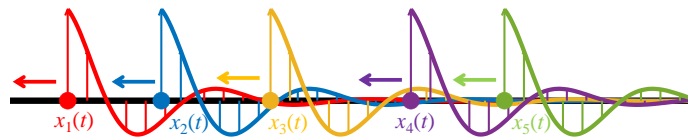


FIG. 1. Schematic of the model (1) for a linear school of flapping swimmers in a fluid. The swimmers are modeled as particles (dots), which are constrained to move in a line to the left. Each swimmer generates a wake whose vertical velocity (curves and arrows) oscillates and decays. These wakes induce horizontal forces on the downstream swimmers, in that a swimmer experiences a horizontal thrust (drag) if it moves up (down) into a downflow or down (up) into an upflow. The interactions between the swimmers are non-reciprocal, as each swimmer is influenced by the wake generated by the swimmers upstream of it.

We here explicitly account for this temporal nonlocality by using a system of nonlinear delay-differential equations to model the wings’ dynamics [34, 38, 39]. The predictions of the model have been shown to exhibit favorable agreement with experiments on flapping wings in a water tank, and with both CFD and vortex sheet simulations of flapping wings [52]. While Viscek-type models with constant time-delay have been studied previously [56, 57], this model differs crucially in that the time-delays are state-dependent [34, 38, 39], which accounts for the fact that the swimmers interact with each other through a fluid-mediated memory. Another key feature of the model is the interactions are non-reciprocal, in that a given swimmer is affected by the flow generated by the swimmers ahead of it. We make two simplifying assumptions: (1) we consider a kinematic model [34], in which the swimmers’ inertia is neglected so hydrodynamic forces directly determine the swimmers’ velocities; and (2) we analyze the model in 1D, thus modeling a linear chain which is perhaps the simplest formation in which fish have been observed to school [58]. By introducing new field variables that account for the persistent vortical flow generated by the swimmers, we show that this model coarse-grains naturally and thus obtain a mean-field continuum PDE description of schooling wings with temporally-nonlocal interactions. We show that, in certain parameter regimes, a uniform-density school of swimmers is unstable to perturbations. These perturbations give rise to traveling waves, which consist of densely populated “sub-schools” of swimmers separated by relatively sparse regions.

II. DERIVATION OF THE CONTINUUM PDE MODEL

We present a derivation of the continuum PDE model, the details of which are given in the Supplemental Material. We consider a collection of N flapping swimmers with positions $x_i(t)$ that self-propel while maintaining an in-line formation (Fig. 1). The swimmers are assumed to

flap in-phase with the same flapping angular frequency ω and amplitude, and are assumed to move to the left, so $\dot{x}_i < 0$. The time-evolution of their positions is governed by a system of nonlinear delay-differential equations, versions of which have been proposed previously to model the hydrodynamic interactions between flapping swimmers in high-Reynolds number flows [34, 38, 39]. The equations are

$$\dot{x}_i = -u_0 - \frac{u_1}{N} \sum_{j=1}^N K(t - t_j(x_i)), \quad (1a)$$

$$\text{where } t_j(x) = \arg_t \{x_j(t) = x\}; \quad (1b)$$

$$K(t) = -H(t)e^{-t/\tau} \cos \omega t; \quad (1c)$$

the constants u_0 , u_1 and η are positive; and $H(t)$ is the Heaviside step function. We have assumed that the swimmers' inertia is negligible and thus the hydrodynamic forces on the swimmers directly determine their velocities.

What do these equations assume and encapsulate? In Eq. (1a), each swimmer is assumed to self-propel in isolation with a speed u_0 , as determined by the balance between hydrodynamic thrust and drag forces on it. The swimmers interact through the term proportional to u_1 , the physical interpretation being that each swimmer experiences hydrodynamic forces due to the vortical wakes generated by each of the upstream swimmers. Following Ref. [38], we employ a simplified description of these wakes: the combined wake is given by a linear superposition of the wakes generated by each swimmer, and the vertical wake speed generated by a given swimmer as it swims by is equal to its instantaneous vertical flapping velocity. This wake speed oscillates in time with frequency ω and decays exponentially over a timescale τ [Eq. (1c)], the latter modeling the turbulent dissipation of flows at high Reynolds number [35, 38, 59, 60]. The force on swimmer i is determined by its vertical velocity relative to the fluid: it experiences a thrust (drag) if it moves up (down) into a downflow or down (up) into an upflow. Equivalently, this force is determined by the swimmer's flapping phase relative to that of its upstream neighbors in the past. This relative phase is accounted for through the time-delays $t_j(x_i)$ defined in Eq. (1b), which specify the time in the past at which swimmer j was in the current position of swimmer i . The non-reciprocal and causal nature of the interactions between swimmers is imposed by the Heaviside function $H(t)$, which ensures that a given swimmer is affected only by the swimmers upstream of it. Taken together, the vorticity-induced hydrodynamic interactions between flapping swimmers in high-Reynolds number flows are reduced to the non-reciprocal interactions of particles through memory: each particle leaves behind a signal, which oscillates and decays in time, and this signal is read by downstream particles as they pass by.

We convert the system of delay-differential equations (1) into a system of ordinary differential equations

by introducing the fields

$$C(x, t) = \frac{1}{N} \sum_{i=1}^N K(t - t_i(x))$$

$$\text{and } S(x, t) = \frac{1}{N} \sum_{i=1}^N \tilde{K}(t - t_i(x)),$$

$$\text{where } \tilde{K}(t) = -H(t)e^{-t/\tau} \sin \omega t. \quad (2)$$

We also make the equations dimensionless via $t \rightarrow t/\tau$ and $x \rightarrow x/(u_0\tau)$, which introduces two dimensionless parameters: the strength of the hydrodynamic interactions $r = u_1/u_0$, and the dimensionless flapping frequency $\alpha = \omega\tau$. Note that

$$\frac{d}{dt}H(t - t_i(x)) = \delta(t - t_i(x)) = \delta(x - x_i(t))|\dot{x}_i|, \quad (3)$$

where the second equality follows from the fact that $\delta(g(z)) = \sum_i \delta(z - z_i)/|g'(z_i)|$ for smooth functions $g(z)$ with roots at $z = z_i$, and the definition $t_i(x_i(t)) = t$. Since $\dot{x}_i < 0$, we can rewrite Eq. (1) as the system

$$\dot{x}_i = -1 - rC(x_i, t), \quad (4a)$$

$$\partial_t C = -\frac{1}{N} \sum_{i=1}^N \delta(x - x_i(t))\dot{x}_i - C - \alpha S, \quad (4b)$$

$$\partial_t S = -S + \alpha C. \quad (4c)$$

The rewriting of Eq. (1) as Eq. (4) is very convenient mathematically, as the temporally-nonlocal hydrodynamic interactions between swimmers (through the time delay functions $t_j(x)$) are replaced by spatial interactions through the aggregated field $C(x, t)$ generated by the swimmers. The oscillatory and decaying nature of the fields C and S (Fig. 1) is evident through the relationship between them in Eqs. (4b)–(4c).

We now seek the mean-field limit of Eq. (4), since we expect that the empirical density $(1/N) \sum_{i=1}^N \delta(x - x_i(t))$ converges to a smooth density $\rho(x, t)$ as $N \rightarrow \infty$. We expect that ρ satisfies the continuity equation $\partial_t \rho + \partial_x(\rho U_0) = 0$ [61, 62], where we define the mean-field swimmer velocity $U_0(x, t) = -1 - rC(x, t)$. Substituting Eq. (4a) into Eq. (4b) and using the fact that $\delta(x - \tilde{x})g(\tilde{x}) = \delta(x - \tilde{x})g(x)$, Eq. (4b) may be rewritten as

$$\partial_t C = \rho U_0 - C - \alpha S. \quad (5)$$

The resulting hyperbolic PDEs admit discontinuous solutions with shocks, so we regularize the equations by replacing $U_0 \rightarrow U_\nu = U_0 - \nu \partial_x(\log \rho)$, where $\nu > 0$ is an effective diffusivity. This additional term modifies the swimmers' velocities to decrease in the presence of a local increase in swimmer density. We thus obtain the equations

$$\partial_t \varrho = \partial_x [(1 + C)\varrho] + \nu \partial_{xx} \varrho, \quad (6a)$$

$$\partial_t C = -\varrho(1 + C) - \nu \partial_x \varrho - C - \alpha S, \quad (6b)$$

$$\partial_t S = -S + \alpha C, \quad (6c)$$

where we rescale the density, $\varrho(x, t) \equiv r\rho(x, t)$, and the fields $C \rightarrow rC$ and $S \rightarrow rS$. Note that the ν -term leads to diffusive contributions in Eq. (6a), which have been proposed in phenomenological PDE models for flocking and schooling [18, 19, 22]. While the swimmers in the biological setting under consideration (e.g. fish) are large enough that thermal fluctuations are insignificant, we hypothesize that random variations in the flapping frequencies, amplitudes or phases may be modeled by such diffusive terms.

Equation (6) constitutes a system of three nonlinear PDEs for the fields $\varrho(x, t)$, $C(x, t)$ and $S(x, t)$. Equation (6a) describes the propagation of swimmer density $\varrho(x, t)$ through hydrodynamic interactions as induced by the field $C(x, t)$ and its diffusion. The field C is generated by the swimmers through the terms proportional to ϱ in Eq. (6b), and is coupled to the field S through Eq. (6c). Through use of the field variables C and S , we have analytically removed the delay terms in Eq. (1), which are otherwise difficult to handle analytically but are crucial for capturing the temporally non-local interactions between swimmers in relatively high-Reynolds number flows. We note that, by introducing the flux $q \equiv -[(1 + C)\varrho + \nu\partial_x\varrho]$ and applying the operator $(\partial_t + 1)$ to Eq. (6c), we can eliminate Eq. (6b) in favor of a second-order equation for S , which highlights the oscillatory dynamics exhibited by S (and, equivalently, C). We opt not to use this mathematically equivalent formulation in the following, as the simplification obtained by eliminating the field variable C is offset by the extra complexity in the evolution equation for S .

III. LINEAR INSTABILITY OF A UNIFORM-DENSITY SCHOOL

The continuum model (6) admits a schooling state of uniform density,

$$\varrho = \varrho_0, \quad C = C_0 \equiv -\frac{\varrho_0}{1 + \alpha^2 + \varrho_0}, \quad S = S_0 \equiv \alpha C_0. \quad (7)$$

The associated swimming speed $1 + C_0$ is a monotonically decreasing function of ϱ_0 , so the swimmers move slower as the density increases. A comparison between the steady states of the discrete [Eq. (1)] and continuum [Eq. (6)] models is given in the Supplemental Material.

We study the linearized behavior of the system near this steady state. The linearized system admits plane-wave solutions, which we demonstrate directly by making the substitution $\varrho(x, t) = \varrho_0 + \epsilon\hat{\varrho}(t)e^{ikx}$, $C(x, t) = C_0 + \epsilon\hat{C}(t)e^{ikx}$ and $S(x, t) = S_0 + \epsilon\hat{S}(t)e^{ikx}$ into Eq. (6) and retaining terms at $O(\epsilon)$. We thus obtain a linear system of ODEs of the form $\dot{\mathbf{z}} = M\mathbf{z}$, where $\mathbf{z} = (\hat{\varrho}, \hat{C}, \hat{S})$ and

$$M(k) = \begin{pmatrix} ik(1 + C_0) - \nu k^2 & ik\varrho_0 & 0 \\ -(1 + C_0) - ik\nu & -(1 + \varrho_0) & -\alpha \\ 0 & \alpha & -1 \end{pmatrix}. \quad (8)$$

Note that the linearized problem depends on the spatial wavenumber k , dimensionless flapping frequency α , diffusivity ν , and rescaled swimmer density ϱ_0 .

We find the three eigenvalues of $M(k)$ numerically, with eigenvalues with (positive) negative real part corresponding to linear (in)stability of the uniform-density schooling state (7). Of the three eigenvalues, we restrict our attention to the one with the largest real part, which we call $s(k)$. The dependence of this eigenvalue on the wavenumber k , for fixed values of the parameters α , ϱ_0 and ν , is shown in Fig. 2a–b. Our numerical computations of this eigenvalue for a range of parameters indicate that, when the uniform state is unstable, it is so for wavenumbers in a single finite interval, $k \in (k_-, k_+)$. Moreover, this eigenvalue has nonzero imaginary part, $\text{Im}(s) > 0$, suggesting that when the uniform-density state is unstable, it destabilizes into a dispersive traveling wave.

In the Supplemental Material we analyze the eigenvalues of $M(k)$ in detail, in order to determine the parameter regimes in which the uniform-density schooling state (7) is unstable. Based on that analysis, we obtain the following results:

1. *Below a critical value of the flapping frequency, $\alpha < \alpha_c(\nu)$, all uniform-density schooling states are stable.*

That is, the uniform-density state can be unstable only if the dimensionless frequency α is sufficiently large:

$$\alpha > \alpha_c(\nu) \equiv \sqrt{\frac{2}{1 - 4\nu(4/3)^3} - 1}. \quad (9)$$

In particular, an instability exists only if the diffusivity is sufficiently small, $\nu < (3/4)^3/4 \approx 0.1$, indicating that large levels of diffusion can eliminate the destabilizing influence of hydrodynamic interactions.

2. *For $\alpha_c(\nu) < \alpha < \alpha^*(\nu)$, uniform-density schooling states with density $\varrho_0 \in (\varrho_-, \varrho_+)$ are unstable. All such states satisfy $k_- = 0$, as depicted in Fig. 2c.*

That is, a long-wave instability occurs as the rescaled density is progressively increased or decreased from the stable regime, $\varrho_0 \uparrow \varrho_-$ or $\varrho_0 \downarrow \varrho_+$. Figure 2c shows the dependence of the perturbation growth rate $\text{Re}(s)$ on the density ϱ_0 and perturbation wavenumber k for a value of α in this regime. The critical densities $\varrho_{\pm}(\alpha, \nu)$, below and above which the uniform-density schooling state is stable, have the following asymptotic expansions in

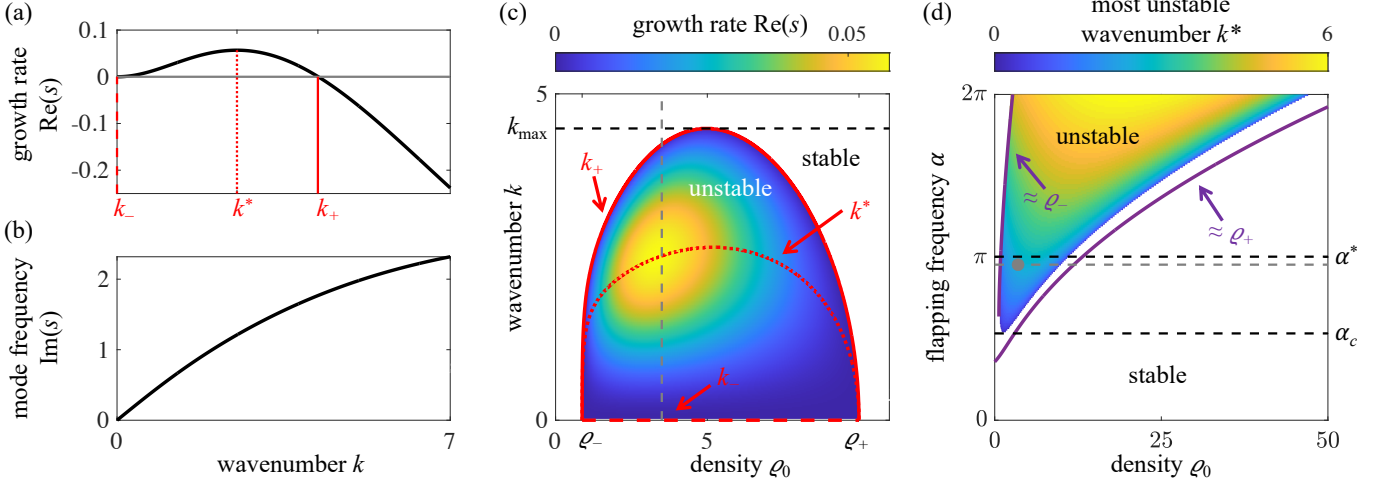


FIG. 2. Results of the linear stability analysis of the uniform-density schooling state, as described in §III. (a–b) Real (a) and imaginary (b) parts of the dominant eigenvalue $s(k)$ of the linear stability problem, for the dimensionless flapping frequency $\alpha = 3$, rescaled density $\rho_0 = 3.5$ and diffusivity $\nu = 0.05$. The uniform state is unstable to perturbations with wavenumbers $k \in (k_-, k_+)$, with $k = k^*$ denoting the wavenumber with the largest growth rate. (c) Growth rate $\text{Re}(s)$ of the dominant eigenvalue, as a function of the school density ρ_0 and perturbation wavenumber k , for $\alpha = 3$ and $\nu = 0.05$. The stable region ($\text{Re}(s) < 0$) is indicated in white. The wavenumbers k_- , k^* and k_+ are indicated by the dashed, dotted and solid red lines, respectively. The vertical gray line corresponds to the density $\rho = 3.5$ used in panels (a)–(b). (d) Most unstable wavenumber k^* as a function of α and ρ , for fixed $\nu = 0.05$. The stable region is again indicated in white. The purple curves show the approximations (10) for the critical densities ρ_{\pm} . The black dashed lines correspond to the critical flapping frequencies α_c and α^* . The gray dot indicates the (ρ_0, α) pair corresponding to panels (a)–(b), and the dashed line denotes the value of α used in panel (c). The value of α used in panels (a)–(c) satisfies $\alpha_c(\nu) < \alpha < \alpha^*(\nu)$; this regime corresponds to scenario #2 described in §III, for which a long-wave instability occurs at $\rho = \rho_{\pm}$.

the limit $\nu \rightarrow 0$:

$$\begin{aligned} \rho_-(\alpha, \nu) &= \frac{\nu(1 + \alpha^2)^2}{\alpha^2 - 1 - 4\nu(\alpha^2 + 1)} + O(\nu^3), \\ \rho_+(\alpha, \nu) &= (\alpha^2 + 1) \left[\left(\frac{\alpha^2 - 1}{\nu(\alpha^2 + 1)} \right)^{1/3} - \frac{4}{3} \right] \\ &\quad + O(\nu^{1/3}). \end{aligned} \quad (10)$$

These asymptotic expressions for $\rho_{\pm}(\alpha, \nu)$ are shown to exhibit good agreement with the numerically computed stability boundary in Fig. 2d. The expressions in Eq. (10) show that, if the rescaled density of swimmers is too low, $\rho_0 < \rho_-$, the hydrodynamic interactions are too weak to overcome the stabilizing influence of diffusion and generate an instability. Conversely, if the density is too large, $\rho_0 > \rho_+$, the diffusion-induced terms proportional to ν in Eq. (6b) cause the hydrodynamic interactions to destructively interfere and thus suppress the instability. Note that, in the limit $\nu \rightarrow 0$, the stability boundaries ρ_- and ρ_+ shown in Fig. 2d become vertical and horizontal lines, respectively, as the uniform-density state would be unstable for any ρ_0 so long as $\alpha > 1$.

- For $\alpha > \alpha^*(\nu)$, uniform-density schooling states with density $\rho_0 \in (\rho_-, \rho_+)$ are unstable. Moreover, there is an intermediate density $\rho^*(\nu) \in (\rho_-, \rho_+)$

above which $k_- = 0$, as in #2, but below which $k_- > 0$.

That is, a *finite*-wavelength instability occurs at relatively low densities, as the density is progressively increased from the stable regime, $\rho_0 \uparrow \rho_-$; but a long-wave instability occurs at relatively high densities, as the density is progressively decreased from the stable regime, $\rho_0 \downarrow \rho_+$ (Supplemental Material). As shown in the Supplemental Material, $\alpha^*(\nu) \rightarrow 1 + \sqrt{2}$ as $\nu \rightarrow 0$.

Figure 2d shows the complete stability diagram for a fixed value of the diffusivity, $\nu = 0.05$, and offers a visualization of the foregoing results. Specifically, it shows the values of density ρ_0 and flapping frequency α for which the uniform-density schooling state is stable (white) and unstable (colored). The colors indicate the most unstable perturbation wavenumber $k^* \in (k_-, k_+)$, defined as the wavenumber for which $\text{Re}(s)$ is the largest (Fig. 2a). The fact that $\text{Im}[s(k^*)] \neq 0$ (Fig. 2b) suggests that the schooling state undergoes a traveling wave instability with a critical length scale $\approx 2\pi/k^*$. We observe from Fig. 2d that k^* increases with α , which indicates that a higher flapping frequency leads to waves with smaller wavelengths. While it is difficult to gain analytical insight into the dependence of k^* on ρ_0 and α , in the Supplemental Material we find a closed form expression for the upper bound k_+ of k^* in the zero-diffusion regime

($\nu = 0$):

$$k_+(\varrho, \alpha) = \frac{(1 + \alpha^2 + \varrho_0)(2 + \varrho_0)}{2(1 + \alpha^2)} \sqrt{\alpha^2 - 1}. \quad (11)$$

It follows from Eq. (11) that k_+ increases with α for $\nu = 0$, in agreement with the trend for k^* observed in Fig. 2d. However, we note that the zero-diffusivity expression (11) predicts that k_+ increases monotonically with ϱ_0 , which is at odds with the non-monotonic dependence of k_+ (and k^*) on ϱ_0 for $\nu > 0$ (Fig. 2c).

The phase and group velocities of the most unstable mode ($k = k^*$) are negative with magnitudes less than unity for all values of α and ϱ_0 , which indicates that the traveling waves propagate in the same direction as, but slower than, an isolated swimmer (Supplemental Material). The phase velocity is larger in magnitude than the group velocity, as is typical for dispersive waves. Moreover, the magnitudes of the phase and group velocities increase with the flapping frequency α but decrease with the density ϱ_0 , which indicates that the waves move faster for larger flapping frequencies but slower for denser schools. The eigenvector $(\hat{\rho}, \hat{C}, \hat{S})$ of $M(k^*)$, which is associated to the most unstable mode, has the property $\arg(\hat{S}) \approx \pi$ throughout the unstable regime (Supplemental Material), where we fix $\hat{\rho} = 1$ without loss of generality. Physically, this means that oscillations in ρ are spatially out-of-phase with those of the field S , or that local increases in the swimmer density correspond to decreases in S . While the other component \hat{C} varies more strongly with respect to ϱ_0 and α (Supplemental Material), we observe that $\arg(\hat{C}) \in (-\pi, -\pi/2)$, indicating that the perturbation in ρ is related to that in C by a phase shift of between a quarter- and half-wavelength.

IV. TRAVELING WAVE SOLUTIONS

The linear stability analysis conducted in §III suggests that the uniform-density schooling state (7) may destabilize through a traveling wave instability. We proceed by confirming the existence of traveling waves by presenting the results of numerical simulations of Eq. (6). As described in the Supplemental Material, we simulate Eq. (6) on a periodic domain of length $2\pi L$ using a pseudospectral method combined with a fourth-order Runge-Kutta time-stepping scheme. We find that, if the initial data are chosen to correspond to the constant-density solution plus a small perturbation (Fig. 3(d,e,f)), the fluctuations in ϱ , C and S grow quite rapidly in time (Fig. 3(g,h,i)), before they saturate into a traveling wave solution of constant speed (Fig. 3(j,k,l)). By comparing Fig. 3(g,j) and Fig. 3(i,l), we observe that ϱ and S are roughly out-of-phase with respect to each other, which is consistent with the linear stability theory in §III.

Supplemental Movie 1 and the spacetime plots in Fig. 3(a,b,c) serve to further illustrate how the uniform-density school destabilizes into a traveling wave. The

“Lagrangian” particles shown in Fig. 3(d,g,j) and Supplemental Movie 1 illustrate the mechanism by which the traveling wave emerges: an initially uniformly distributed collection of swimmers destabilizes into a collection of densely populated “sub-schools” separated by relatively sparse regions. The leader of one of the sub-schools accelerates into the rear of the upstream sub-school, a process that continues periodically and thus generates a moving wave.

In order to systematically characterize the traveling wave solutions to Eq. (6), we substitute the expressions $\varrho(x, t) = \varrho(x + ct)$, $C(x, t) = C(x + ct)$ and $S(x, t) = S(x + ct)$, where the wave profiles ϱ , C and S satisfy a system of nonlinear ODEs with periodic boundary conditions:

$$\begin{aligned} c\rho' - [(1 + C)\varrho]' - \nu\varrho'' &= 0, \\ cC' + \varrho(1 + C) + \nu\varrho' + C + \alpha S &= 0, \\ cS' + S - \alpha C &= 0. \end{aligned} \quad (12)$$

Equation (12) constitutes a nonlinear eigenvalue problem in the wave speed c . We discretized the ODEs using a pseudospectral method, and then used MATLAB’s root-finding algorithm to solve the resulting system of algebraic equations. Using the numerical method described in the Supplemental Material, the traveling wave solutions were systematically tracked as a function of the density $\varrho_0 = \langle \varrho \rangle$ for fixed values of the flapping frequency α and diffusivity ν , where $\langle \cdot \rangle$ denotes a spatial average. The solutions are characterized by their amplitude $A = \sqrt{2\langle \varrho^2 \rangle}$ and wave speed c , which are plotted as functions of ϱ_0 in Fig. 4(a,b).

As shown in Fig. 4a, for fixed values of α and ν , a (finite) family of $n_{\max} = \lfloor k_{\max} L \rfloor$ solution branches exists, where $k_{\max} = \max_{\varrho_0} k_+(\varrho_0)$ is the largest unstable wavenumber across all densities ϱ_0 (Fig. 2c). The branches may be indexed by the number of minima n in the wave profiles ϱ , for $1 \leq n \leq n_{\max}$ (Fig. 4, bottom panels). Specifically, the $n = 1$ branch corresponds to states of roughly constant density, punctuated by a single exponentially localized vacancy. The density profile of the vacancy is asymmetric about its minimum value, exhibiting a sharper gradient upstream (left) than downstream (right). As n increases, the characteristic distance between high-density sub-schools decreases. The wave speed c is less than unity (Fig. 4b), indicating that the traveling waves move slower than a single isolated swimmer, which is consistent with the linear stability theory presented in §III (Supplemental Material). Similarly, the wave speed decreases with n , indicating that schools with a large number of density fluctuations move slower than relatively uniform ones. As the domain length $L \rightarrow \infty$, the diagram in Fig. 4a will be populated by an infinite family of solutions, which we expect to effectively fill in the region bounded by the solution branches shown.

Not all of the traveling wave solutions shown in Fig. 4 are stable. To assess their stability, we perform numerical simulations of the continuum PDE (6) up to the dimensionless time $t = 5000$, with initial conditions given

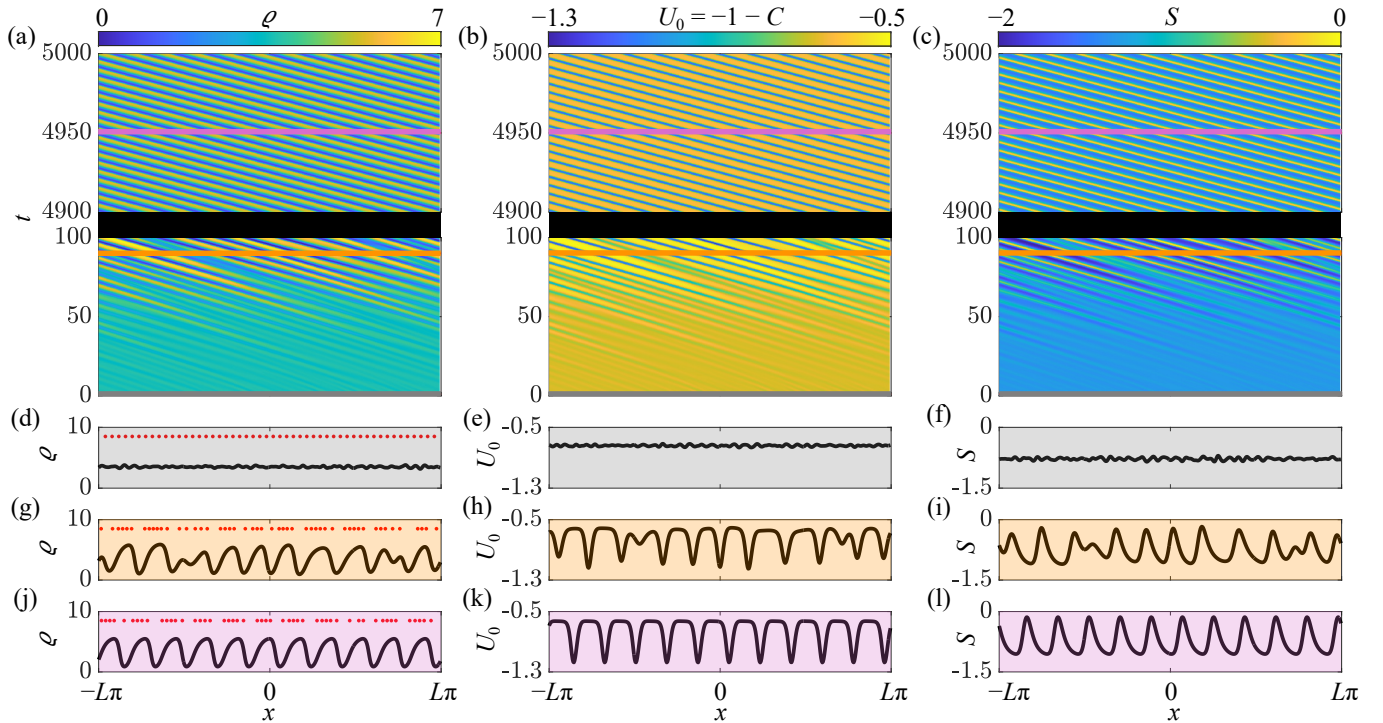


FIG. 3. Numerical simulation of Eq. (6) shows how small perturbations to a uniform-density schooling state amplify into a self-sustaining traveling wave. The parameters are the initial density $\varrho_0 = 3.5$, dimensionless flapping frequency $\alpha = 3$, diffusivity $\nu = 0.05$ and domain size $2\pi L$ where $L = 5$. (a–c) Spacetime plots of the density ϱ (panel a) and fields $U_0 = -1 - C$ (panel b) and S (panel c). (d–o) Snapshots of the solution at three distinct times t , indicated by the horizontal lines in panels (a–c) and color-coded appropriately. The density ϱ is shown in panels (d,g,j), U_0 in (e,h,k) and S in (f,i,l). Panels (d,g,j) also illustrate the evolving density using “Lagrangian” particles that satisfy the ODEs $\dot{x}_i = U_0(x_i, t)$, with initial conditions $x_i(0)$ uniformly distributed on the interval shown. A movie of this solution is in Supplemental Movie 1.

by the traveling waves shown in Fig. 4, and determine whether the initial traveling wave persists. The results are shown in Fig. 5, with stable (unstable) solutions indicated in blue (red). Figure 5b shows that highly oscillatory traveling waves, with relatively large wavenumbers $k_n \equiv n/L$, are typically unstable. Low wavenumber waves are also typically unstable, except at the highest swimmer densities ϱ_0 . We observe that multiple stable traveling waves may coexist for the same density ϱ_0 , indicating that linear schools may exhibit different stable wave modes. The most unstable wavenumber k^* , as predicted by the linear stability analysis in §III (Fig. 2c), lies inside the region of stability for traveling waves (Fig. 5b). We conclude that, for a fixed density ϱ_0 , the most (linearly) unstable wavenumber k^* furnishes a reasonable prediction for the wavenumbers k_n of the stable traveling waves that exist for that density. We also note that, for some of the branches at low n (i.e. $n = 1$), the amplitude A is not a single-valued function of the density ϱ_0 for large ϱ_0 . Indeed, some of these branches extend to the right of the linear stability boundary $\varrho = \varrho_+$ (Fig. 5a): while the corresponding uniform-density schooling states (7) are stable under infinitesimally small perturbations in this regime, they may destabilize under the influence of finite-amplitude perturbations.

We note that the value $\alpha = 3$ considered in Fig. 4 and Fig. 5 corresponds roughly to that found by Newbolt *et al.* [38] in their experiments on tandem flapping wings in a water tank. Specifically, they measured a decay time $\tau \approx 0.5$ s and considered wings with flapping frequency $f \approx 2$ Hz, for which $\alpha \approx 6$. We find qualitatively similar traveling wave solutions for a range of values of α and ν .

V. DISCUSSION

In this paper, we derived and analyzed a continuum model for schooling swimmers that accounts for interactions via a fluid-mediated memory. The dynamics of the swimmers is governed by a system of nonlinear delay-differential equations (Eq. (1)), versions of which have previously been benchmarked against experimental [34, 38, 39] and numerical [52] studies on schooling wings. The interactions between swimmers have two salient features: they are non-reciprocal, in that a given swimmer is affected only by those upstream of it; and they are temporally nonlocal, in that they are determined by the relative phases of a given swimmer’s flapping motion and that of the other swimmers in the past. By introducing the new field variables C and S , which account for

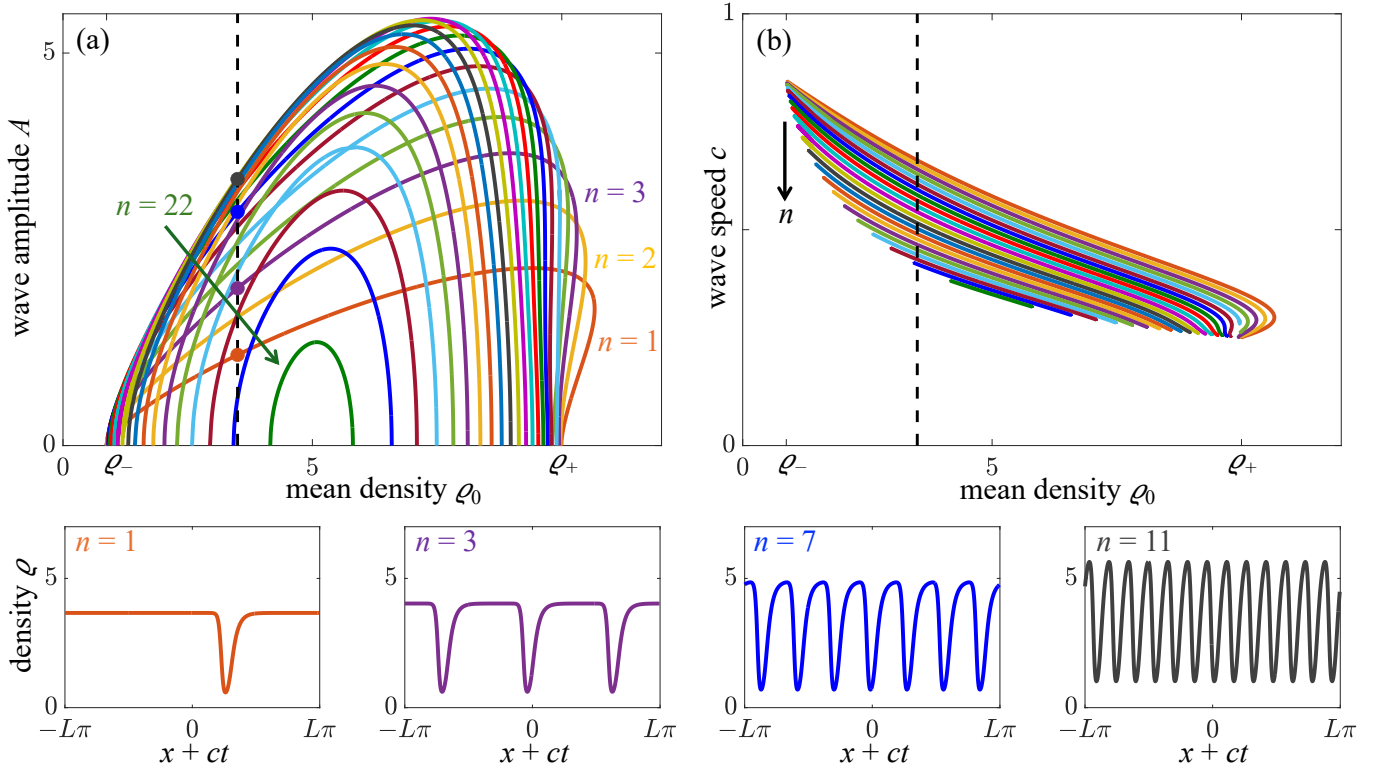


FIG. 4. Traveling wave solutions to the continuum PDE model (6) for schooling swimmers, for the dimensionless flapping frequency $\alpha = 3$, diffusivity $\nu = 0.05$ and domain size $2\pi L$ where $L = 5$. The solutions are computed by solving the nonlinear eigenvalue problem (12) using the numerical procedure described in the Supplemental Material. Panels (a) and (b) show the dependence of the wave amplitude A and speed c on the mean density ϱ_0 , respectively. The branches are color-coded by their index n , which indicates the number of minima in the corresponding density profiles. The bottom panels show four density profiles for a fixed mean density $\varrho_0 = 3.5$, with the indicated values of n .

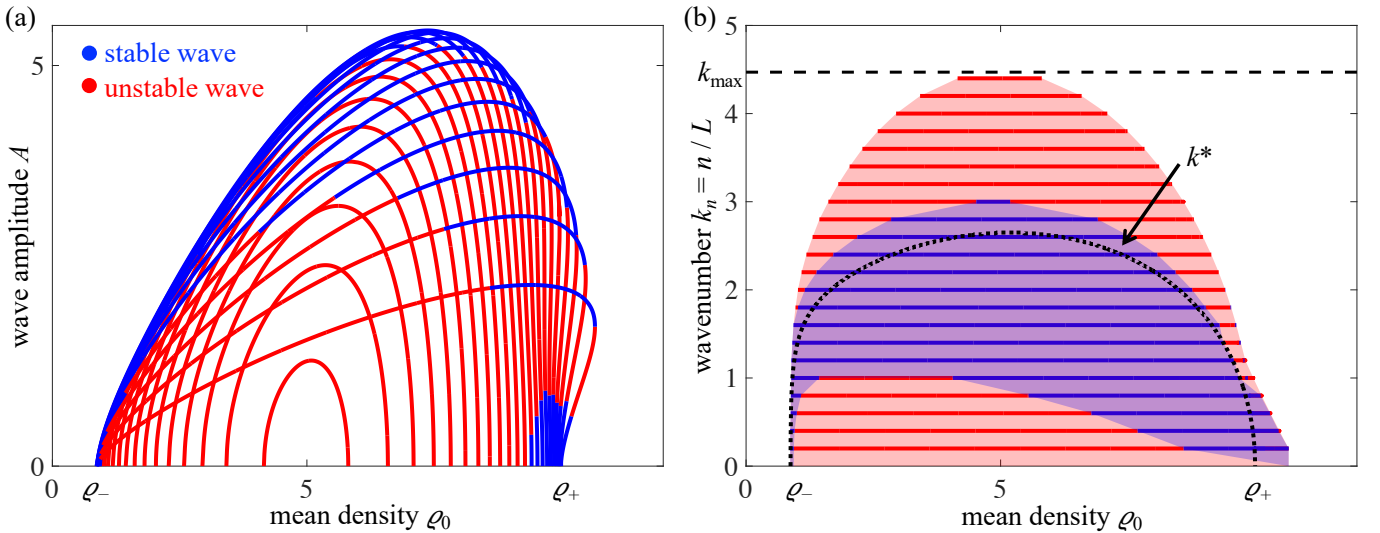


FIG. 5. Stability of the traveling wave solutions shown in Fig. 4. Blue (red) denote stable (unstable) solutions. (a) Traveling wave solutions shown in Fig. 4a, now color-coded according to their stability. (b) Stability diagram of traveling wave solutions, obtained by taking the results in panel (a) and recasting them in terms of the solution's wavenumber $k_n \equiv n/L$. A point (ϱ_0, k_n) is colored blue if at least one stable solution exists, and red otherwise. The black curve indicates the prediction of the most unstable wavenumber k^* (Fig. 2c) based on the linear stability analysis presented in §III.

the oscillatory and decaying nature of these interactions, we coarse-grained the system analytically and obtained a mean-field PDE theory (6) that we expect to be valid in the limit of a large number of swimmers, $N \rightarrow \infty$.

Linear stability analysis of the PDE reveals that a uniform-density schooling state is unstable in an intermediate range of densities, $\varrho_0 \in (\varrho_-, \varrho_+)$, provided that the dimensionless flapping frequency α is sufficiently large, $\alpha > \alpha_c$ (Fig. 2). Both long-wave and finite-wavelength instabilities can occur for $\varrho_0 = \varrho_-$, and long-wave instabilities occur for $\varrho_0 = \varrho_+$ (Supplemental Material). The unstable states destabilize into traveling waves, wherein densely populated “sub-schools” are separated by relatively sparse regions (Fig. 3). A systematic characterization of these traveling waves reveals that they exist as distinct solution branches across a range of swimmer densities ϱ_0 (Fig. 4a), with a given branch n indicating the number of oscillations in the swimmer density profile. The traveling wave speed c typically decreases with both the number of oscillations n and the mean density ϱ_0 (Fig. 4b). Numerical simulations of the PDE (6) reveal that, while not all of these traveling wave solutions are stable, multiple stable traveling wave solutions may coexist for identical values of the mean density ϱ_0 , dimensionless flapping frequency α and diffusivity ν (Fig. 5).

Traveling waves have been observed in many other models for self-propelled particles. For example, the Viscek model exhibits density waves [63], which arise through microphase separation between relatively low and high density regions [64]. The density waves may coexist with the homogenous isotropic state [65], which is qualitatively similar to the observation from our model that stable traveling waves may coexist with the uniform-density schooling state for $\varrho_0 > \varrho_+$ (Fig. 5a). The traveling waves observed in our model also bear some resemblance to those exhibited in a model of chemotactic motility-induced phase separation (MIPS): unlike conventional MIPS where there is no directional bias [66], systems that chemotax exhibit persistent directed motion in a given direction, and are observed to phase separate into bands that form traveling waves in certain parameter regimes [67]. Similarly, the swimmers in our model move with a fixed velocity $-u_0$ in isolation, and the traveling waves exhibited by the collective can be interpreted as a sort of phase separation between dilute and dense phases. Traveling waves have also been observed in phenomenological flocking models that consist of partial integro-differential equations with both symmetric [23] and asymmetric [68] interactions, the latter being more reminiscent of the non-reciprocal interactions encoded in our model (1). Wave-like behavior has also been observed in experimental [39] and numerical [52, 53] studies of in-line formations of relatively small collectives of flapping wings, wherein disturbances to the leader wing propagate downstream and lead to collisions between the trailing wings.

Hydrodynamic interactions have been observed to in-

duce traveling wave behavior in other biological active matter systems, for instance in microswimmers [69, 70], cilia [55, 71–74] and algae [75, 76] at low Reynolds numbers, and in nematode collectives at intermediate Reynolds numbers [77, 78]. However, our work is a theoretical demonstration of traveling wave behavior in a system governed by the high-Reynolds number hydrodynamic interactions characteristic of fish schools and bird flocks. Turning waves have been observed in bird flocks [79] and shimmering waves in fish schools [80], the latter being a visual manifestation of the escape waves exhibited by schooling fish in response to attack by a predator [81, 82]. While our model entirely neglects behavioral mechanisms, the hydrodynamics-induced traveling wave instability we have identified could complement other wave-like phenomena driven by behavior. To probe the interplay between hydrodynamics and behavior, one could extend the model to allow the swimmers to sense both each other [42] and hydrodynamic pressure forces [83, 84], as fish are thought to respond behaviorally to such cues in natural settings. Generalizations of the theory in which the swimmers move in three dimensions while changing their swimming direction might be used to model collectives with more complex internal structure.

The main predictions of our continuum theory are that schooling swimmers in a linear formation exhibit traveling waves whose speed decreases both with the mean density and the number of density oscillations, which could be tested in experimental or observational studies of fish schools. Moreover, we presume that sufficiently strong external perturbations to a fish school could induce switching between the different multistable traveling wave modes, an effect that could be important in rationalizing the complex dynamics exhibited by fish schools. Incorporating the swimmers’ inertia into the model could lead to modulational and other more complex instabilities. Inertial effects are thought to be relevant in understanding the dynamics of bird flocks [85–87], and have been shown to have significantly influence the dynamics of certain active matter systems [88]. These worthwhile future directions would build on the modeling and analytical techniques presented herein, which provide a general framework for incorporating fluid-mediated memory into a continuum theory for active matter systems.

ACKNOWLEDGMENTS

We thank Leif Ristroph and Miles Wheeler for useful discussions. A.U.O. acknowledges support from NSF DMS-2108839. Funding to E.K. is provided by the NSF grants RAISE IOS-2034043 and CBET-210020 and the Office of Naval Research grants N00014-22-1-2655 and N00014-19-1-2035.

- [1] D. S. Pavlov and A. O. Kasumyan. Patterns and mechanisms of schooling behavior in fish: A review. *J. Ichthyology*, 40:S163–S231, 2000.
- [2] M. C. Marchetti, J. F. Joanny, S. Ramaswamy, T. B. Liverpool, J. Prost, M. Rao, and R. A. Simha. Hydrodynamics of soft active matter. *Reviews of Modern Physics*, 85(1143), 2013.
- [3] E. Shaw. The schooling of fishes. *Scientific American*, 206(6):128–141, 1962.
- [4] B. L. Partridge. The structure and function of fish schools. *Scientific American*, 246(6):114–123, 1982.
- [5] J. D. Geder, R. Ramamurti, D. Edwards, T. Young, and M. Pruessner. Development of an unmanned hybrid vehicle using artificial pectoral fins. *Marine Technology Society Journal*, 51(56), 2017.
- [6] J. K. Parrish, S. V. Viscido, and D. Grünbaum. Self-organized fish schools: An examination of emergent properties. *The Biological Bulletin*, 202(3):296–305, 2002.
- [7] U. Lopez, J. Gautrais, I. D. Couzin, and G. Theraulaz. From behavioural analyses to models of collective motion in fish schools. *Interface Focus*, 218:1–11, 2012.
- [8] J. W. Jolles, N. J. Boogert, V. H. Sridhar, I. D. Couzin, and A. Manica. Consistent individual differences drive collective behavior and group functioning of schooling fish. *Current Biology*, 27:2862–2868, 2017.
- [9] K. Tunström, Y. Katz, C. C. Ioannou, C. Huepe, M. J. Lutz, and I. D. Couzin. Collective states, multistability and transitional behavior in schooling fish. *PLOS Computational Biology*, 9(2):e1002915, 2013.
- [10] J. Gautrais, F. Ginelli, R. Fournier, S. Blanco, M. Soria, H. Chaté, and G. Theraulaz. Deciphering interactions in moving animal groups. *PLOS Computational Biology*, 8(9):1–11, 09 2012.
- [11] Y. Katz, K. Tunström, C. C. Ioannou, C. Huepe, and I. D. Couzin. Inferring the structure and dynamics of interactions in schooling fish. *Proceedings of the National Academy of Sciences*, 108(46):18720–18725, 2011.
- [12] J. E. Herbert-Read, A. Perna, R. P. Mann, T. M. Schaefer, D. J. T. Sumpter, and A. J. W. Ward. Inferring the rules of interaction of shoaling fish. *Proceedings of the National Academy of Sciences*, 108(46):18726–18731, 2011.
- [13] Y. Yang, F. Turci, E. Kague, C. L. Hammond, J. Russo, and C. P. Royall. Dominating lengthscales of zebrafish collective behaviour. *PLOS Computational Biology*, 18(1):1–14, 01 2022.
- [14] T. Vicsek, A. Czirók, E. Ben-Jacob, I. Cohen, and O. Shochet. Novel type of phase transition in a system of self-driven particles. *Physical Review Letters*, 75(6), 1995.
- [15] A. Huth and C. Wissel. The simulation of the movement of fish schools. *Journal of Theoretical Biology*, 156:365–385, 1992.
- [16] H. Chaté, F. Ginelli, G. Grégoire, F. Peruani, and F. Raynaud. Modeling collective motion: variations on the Vicsek model. *Eur. Phys. J. B*, 64:451–456, 2008.
- [17] D. S. Calovi, U. Lopez, P. Schuhmacher, H. Chaté, C. Sire, and G. Theraulaz. Collective response to perturbations in a data-driven fish school model. *J. R. Soc. Interface*, 12, 2015.
- [18] J. Toner and Y. Tu. Flocks, herds and schools: A quantitative theory of flocking. *Phys. Rev. E*, 58(4828), 1998.
- [19] J. Toner and Y. Tu. Long-range order in a two-dimensional dynamical XY model: How birds fly together. *Physical Review Letters*, 75(23), 1995.
- [20] J. Toner. Reanalysis of the hydrodynamic theory of fluid, polar-ordered flocks. *Physical Review E*, 86(031918), 2012.
- [21] A. Cavagna, I. Giardina, T. S. Grigera, A. Jelić, D. Levine, S. Ramaswamy, and M. Viale. Silent flocks: Constraints on signal propagation across biological groups. *Physical Review Letters*, 114(218101), 2015.
- [22] X. Yang and M. C. Marchetti. Hydrodynamics of turning flocks. *Physical Review Letters*, 115(258101), 2015.
- [23] A. Mogilner and L. Edelstein-Keshet. A non-local model for a swarm. *Journal of Mathematical Biology*, 38:534–570, 1999.
- [24] C. M. Topaz and A. L. Bertozzi. Swarming patterns in a two-dimensional kinematic model for biological groups. *SIAM Journal of Applied Mathematics*, 65(1):152–174, 2004.
- [25] J. A. Carrillo, S. Martin, and V. Panferov. A new interaction potential for swarming models. *Physica D*, 260:112–126, 2013.
- [26] A. J. Leverentz, C. M. Topaz, and A. J. Bernoff. Asymptotic dynamics of attractive-repulsive swarms. *SIAM Journal on Applied Dynamical Systems*, 8(3):880–908, 2009.
- [27] M. S. Triantafyllou, G. S. Triantafyllou, and D. K. P. Yue. Hydrodynamics of fishlike swimming. *Annual Review of Fluid Mechanics*, 32:33–53, 2000.
- [28] M. Ligman, J. Lund, and M. Fürth. A comprehensive review of hydrodynamic studies on fish schooling. *Bioinspiration & Biomimetics*, 19(1):011002, 2023.
- [29] S. Marras, S. S. Killen, J. Lindström, D. J. McKenzie, J. F. Steffensen, and P. Domenici. Fish swimming in schools save energy regardless of their spatial position. *Behavioral Ecology and Sociobiology*, 69:219–226, 2015.
- [30] J. Herskin and J. F. Steffensen. Energy savings in sea bass swimming in a school: measurements of tail beat frequency and oxygen consumption at different swimming speeds. *Journal of Fish Biology*, 53:366–376, 1998.
- [31] Y. Zhang and G. V. Lauder. Energy conservation by collective movement in schooling fish. *eLife*, 12(RP90352), 2024.
- [32] Y. Zhang, H. Ko, M. A. Calicchia, R. Ni, and G. V. Lauder. Collective movement of schooling fish reduces the costs of locomotion in turbulent conditions. *PLOS Biology*, 22(6):1–28, 06 2024.
- [33] I. Ashraf, H. Bradshaw, T.-T. Ha, J. Halloy, R. Godoy-Diana, and B. Thiria. Simple phalanx pattern leads to energy saving in cohesive fish schooling. *Proceedings of the National Academy of Sciences*, 114(36):9599–9604, 2017.
- [34] A. D. Becker, H. Masoud, J. W. Newbolt, M. Shelley, and L. Ristroph. Hydrodynamic schooling of flapping swimmers. *Nat. Commun.*, 6(8514), 2015.
- [35] S. Ramanananarivo, F. Fang, A. Oza, J. Zhang, and L. Ristroph. Flow interactions lead to orderly formations of flapping wings in forward flight. *Phys. Rev. Fluids*, 1(071201(R)), 2016.
- [36] J. W. Newbolt, J. Zhang, and L. Ristroph. Lateral flow interactions enhance speed and stabilize formations of flapping swimmers. *Phys. Rev. Fluids*, 7:L061101, 2022.

- [37] P. C. Ormonde, M. Kurt, A. Mivehchi, and K. W. Moored. Two-dimensionally stable self-organisation arises in simple schooling swimmers through hydrodynamic interactions. *Journal of Fluid Mechanics*, 1000:A90, 2024.
- [38] J. W. Newbolt, J. Zhang, and L. Ristroph. Flow interactions between uncoordinated flapping swimmers give rise to group cohesion. *Proc. Natl. Acad. Sci. USA*, 116(9):2419–2424, 2019.
- [39] J. W. Newbolt, N. Lewis, M. Bleu, J. Wu, C. Mavroyiakoumou, S. Ramanarivo, and L. Ristroph. Flow interactions lead to self-organized flight formations disrupted by self-amplifying waves. *Nature Communications*, 15:3462, 2024.
- [40] A. C. H. Tsang and E. Kanso. Dipole interactions in doubly periodic domains. *Journal of Nonlinear Science*, 23(6):971–991, 2013.
- [41] M. Gazzola, A. A. Tchieu, D. Alexeev, A. de Brauer, and P. Koumoutsakos. Learning to school in the presence of hydrodynamic interactions. *Journal of Fluid Mechanics*, 789:726–749, 2016.
- [42] A. Filella, F. Nadal, C. Sire, E. Kanso, and C. Eloy. Model of collective fish behavior with hydrodynamic interactions. *Physical Review Letters*, 120(198101), 2018.
- [43] C. Huang, F. Ling, and E. Kanso. Collective phase transitions in confined fish schools. *Proceedings of the National Academy of Sciences*, 121(44):e2406293121, 2024.
- [44] T. Y. Wu. Swimming of a waving plate. *J. Fluid Mech.*, 10(03):321–344, 1961.
- [45] T. Y. Wu and A. T. Chwang. Extraction of flow energy by fish and birds in a wavy stream. In *Swimming and flying in nature*, pages 687–702. Springer, 1975.
- [46] P. J. Baddoo, N. J. Moore, A. U. Oza, and D. G. Crowdy. Generalization of waving-plate theory to multiple interacting swimmers. *Communications on Pure and Applied Mathematics*, 76(12):3811–3851, 2023.
- [47] D. Weihs. Hydromechanics of fish schooling. *Nature*, 241, 1973.
- [48] D. Weihs. Some hydrodynamical aspects of fish schooling. In T. Y. Wu, C. J. Brokaw, and C. Brennen, editors, *Swimming and Flying in Nature*, pages 703–718. Springer, 1975.
- [49] A. U. Oza, L. Ristroph, and M. J. Shelley. Lattices of hydrodynamically interacting flapping swimmers. *Physical Review X*, 9(041024), 2019.
- [50] S. Heydari and E. Kanso. School cohesion, speed and efficiency are modulated by the swimmers flapping motion. *Journal of Fluid Mechanics*, 922:A27, 2021.
- [51] F. Fang, C. Mavroyiakoumou, L. Ristroph, and M. J. Shelley. Flow interactions and forward flight dynamics of tandem flapping wings, 2025.
- [52] S. Heydari, H. Hang, and E. Kanso. Mapping spatial patterns to energetic benefits in groups of flow-coupled swimmers. *eLife*, 13(RP96129), 2024.
- [53] M. Nitsche, A. U. Oza, and M. Siegel. On the stability of an in-line formation of hydrodynamically interacting flapping plates. *Journal of Fluid Mechanics*, 1013:A14, 2025.
- [54] D. Saintillan and M. Shelley. Emergence of coherent structures and large-scale flows in motile suspensions. *J. R. Soc. Interface*, 9(68):571–585, 2011.
- [55] R. Golestanian, J. M. Yeomans, and N. Uchida. Hydrodynamic synchronization at low Reynolds number. *Soft Matter*, 7:3074–3082, 2011.
- [56] E. Forgoston and I. B. Schwartz. Delay-induced instabilities in self-propelling swarms. *Phys. Rev. E*, 77:035203, Mar 2008.
- [57] V. Holubec, D. Geiss, S. A. M. Loos, K. Kroy, and F. Cichos. Finite-size scaling at the edge of disorder in a time-delay vicsek model. *Phys. Rev. Lett.*, 127:258001, 2021.
- [58] E. W. Gudger. Fishes that swim heads to tails in single file. *Copeia*, 1944(3):152–154, 1944.
- [59] J. J. L. Higdon and S. Corrsin. Induced drag of a bird flock. *The American Naturalist*, 112(986):727–744, 1978.
- [60] M. Daghooghi and I. Borazjani. The hydrodynamic advantages of synchronized swimming in a rectangular pattern. *Bioinspiration and Biomimetics*, 10(056018), 2015.
- [61] F. Golse. On the dynamics of large particle systems in the mean field limit. In A. Muntean, J. Rademacher, and A. Zagaris, editors, *Macroscopic and Large Scale Phenomena: Coarse Graining, Mean Field Limits and Ergodicity*, pages 1–144. Springer International Publishing, Cham, 2016.
- [62] P.-E. Jabin and Z. Wang. Mean field limit for stochastic particle systems. In N. Bellomo, P. Degond, and E. Tadmor, editors, *Active Particles, Volume 1 : Advances in Theory, Models, and Applications*, pages 379–402. Springer International Publishing, Cham, 2017.
- [63] G. Grégoire and H. Chaté. Onset of collective and cohesive motion. *Phys. Rev. Lett.*, 92:025702, 2004.
- [64] A. P. Solon, H. Chaté, and J. Tailleur. From phase to microphase separation in flocking models: The essential role of nonequilibrium fluctuations. *Phys. Rev. Lett.*, 114:068101, 2015.
- [65] J.-B. Caussin, A. Solon, A. Peshkov, H. Chaté, T. Dauxois, J. Tailleur, V. Vitelli, and D. Bartolo. Emergent spatial structures in flocking models: A dynamical system insight. *Phys. Rev. Lett.*, 112:148102, 2014.
- [66] M. E. Cates and J. Tailleur. Motility-induced phase separation. *Annual Review of Condensed Matter Physics*, 6(Volume 6, 2015):219–244, 2015.
- [67] H. Zhao, A. Košmrlj, and S. S. Datta. Chemotactic motility-induced phase separation. *Phys. Rev. Lett.*, 131:118301, Sep 2023.
- [68] P. A. Milewski and X. Yang. A simple model for biological aggregation with asymmetric sensing. *Communications in Mathematical Sciences*, 6(2), 2008.
- [69] A. C. H. Tsang and E. Kanso. Density shock waves in confined microswimmers. *Phys. Rev. Lett.*, 116:048101, Jan 2016.
- [70] A. C. H. Tsang, M. J. Shelley, and E. Kanso. Activity-induced instability of phonons in 1D microfluidic crystals. *Soft Matter*, 14:945–950, 2018.
- [71] C. Wollin and H. Stark. Metachronal waves in a chain of rowers with hydrodynamic interactions. *The European Physical Journal E*, 34(4):42, 2011.
- [72] F. Meng, R. R. Bennett, N. Uchida, and R. Golestanian. Conditions for metachronal coordination in arrays of model cilia. *Proceedings of the National Academy of Sciences*, 118(32):e2102828118, 2021.
- [73] A. V. Kanale, F. Ling, H. Guo, S. Fürthauer, and E. Kanso. Spontaneous phase coordination and fluid pumping in model ciliary carpets. *Proceedings of the National Academy of Sciences*, 119(45):e2214413119, 2022.
- [74] B. Chakrabarti, S. Fürthauer, and M. J. Shelley. A multiscale biophysical model gives quantized metachronal waves in a lattice of beating cilia. *Proceedings of the National Academy of Sciences*, 119(4):e2113539119, 2022.

- [75] D. R. Brumley, M. Polin, T. J. Pedley, and R. E. Goldstein. Hydrodynamic synchronization and metachronal waves on the surface of the colonial alga *volvox carteri*. *Phys. Rev. Lett.*, 109:268102, Dec 2012.
- [76] D. R. Brumley, M. Polin, T. J. Pedley, and R. E. Goldstein. Metachronal waves in the flagellar beating of *volvox* and their hydrodynamic origin. *Journal of The Royal Society Interface*, 12(108):20141358, 2015.
- [77] A. C. Quillen, A. Peshkov, E. Wright, and S. McGaffigan. Metachronal waves in concentrations of swimming turbotratrix aceti nematodes and an oscillator chain model for their coordinated motions. *Phys. Rev. E*, 104:014412, Jul 2021.
- [78] A. Peshkov, S. McGaffigan, and A. C. Quillen. Synchronized oscillations in swarms of nematode turbotratrix aceti. *Soft Matter*, 18:1174–1182, 2022.
- [79] W. K. Potts. The chorus-line hypothesis of manoeuvre coordination in avian flocks. *Nature*, 309(5966):344–345, 1984.
- [80] A. Pertzalan, G. Ariel, and M. Kiflawi. Schooling of light reflecting fish. *PLOS ONE*, 18(7):1–20, 07 2023.
- [81] J. E. Herbert-Read, C. Buhl, F. Hu, A. J. W. Ward, and D. J. T. Sumpter. Initiation and spread of escape waves within animal groups. *R. Soc. Open Sci.*, 2:140355, 2015.
- [82] W. Poel, B. C. Daniels, M. M. G. Sosna, C. R. Twomey, S. P. Leblanc, I. D. Couzin, and P. Romanczuk. Subcritical escape waves in schooling fish. *Science Advances*, 8(25):eabm6385, 2022.
- [83] J. C. Liao. A review of fish swimming mechanics and behaviour in altered flows. *Phil. Trans. R. Soc. B*, 362:1973–1993, 2007.
- [84] L. Ristroph, J. C. Liao, and J. Zhang. Lateral line layout correlates with the differential hydrodynamic pressure on swimming fish. *Physical Review Letters*, 114(018102), 2015.
- [85] A. Attanasi, A. Cavagna, L. D. Castello, I. Giardina, T. S. Grigera, A. Jelić, S. Melillo, L. Parisi, O. Pohl, E. Shen, and M. Viale. Information transfer and behavioural inertia in starling flocks. *Nature Physics*, 10:691–696, 2014.
- [86] A. Cavagna, L. D. Castello, I. Giardina, T. Grigera, A. Jelic, S. Melillo, T. Mora, L. Parisi, E. Silvestri, M. Viale, and A. M. Walczak. Flocking and turning: a new model for self-organized collective motion. *Journal of Statistical Physics*, 158(3):601–627, 2015.
- [87] A. Cavagna, D. Conti, C. Creato, L. D. Castello, I. Giardina, T. S. Grigera, S. Melillo, L. Parisi, and M. Viale. Dynamic scaling in natural swarms. *Nature Physics*, 13(9):914–918, 2017.
- [88] H. Löwen. Inertial effects of self-propelled particles: From active Brownian to active Langevin motion. *The Journal of Chemical Physics*, 152(4):040901, 2020.